

# Circulating but not immobilized N-deglycosylated von Willebrand factor increases platelet adhesion under flow conditions

Cite as: Biomicrofluidics 7, 044124 (2013); <https://doi.org/10.1063/1.4819746>

Submitted: 20 July 2013 • Accepted: 13 August 2013 • Published Online: 26 August 2013

M. A. Fallah, V. Huck, V. Niemeyer, et al.



View Online



Export Citation



CrossMark

## ARTICLES YOU MAY BE INTERESTED IN

[Field tested milliliter-scale blood filtration device for point-of-care applications](#)

Biomicrofluidics 7, 044111 (2013); <https://doi.org/10.1063/1.4817792>

[Sorting of circulating tumor cells \(MV3-melanoma\) and red blood cells using non-inertial lift](#)

Biomicrofluidics 7, 044120 (2013); <https://doi.org/10.1063/1.4818907>

[Vortex-aided inertial microfluidic device for continuous particle separation with high size-selectivity, efficiency, and purity](#)

Biomicrofluidics 7, 044119 (2013); <https://doi.org/10.1063/1.4818906>



Biophysics Reviews

First Articles Now Online!

READ NOW >>>





## Circulating but not immobilized N-deglycosylated von Willebrand factor increases platelet adhesion under flow conditions

M. A. Fallah,<sup>1,2,a)</sup> V. Huck,<sup>3,a)</sup> V. Niemeyer,<sup>3</sup> A. Desch,<sup>3</sup> J. I. Angerer,<sup>1</sup>  
T. A. J. McKinnon,<sup>4</sup> A. Wixforth,<sup>1</sup> S. W. Schneider,<sup>3,b)</sup> and M. F. Schneider<sup>5,b)</sup>

<sup>1</sup>University of Augsburg, Chair of Experimental Physics I, 86159 Augsburg, Germany

<sup>2</sup>Department of Biophysical Chemistry, University of Konstanz, 78457 Konstanz, Germany

<sup>3</sup>Heidelberg University, Medical Faculty Mannheim, Experimental Dermatology, 68167 Mannheim, Germany

<sup>4</sup>Imperial College London, Hammersmith Hospital Campus, Department of Medicine, London W12 0NN, United Kingdom

<sup>5</sup>Department of Mechanical Engineering, Boston University, Boston, Massachusetts 02215, USA

(Received 20 July 2013; accepted 13 August 2013; published online 26 August 2013)

The role of von Willebrand factor (VWF) as a shear stress activated platelet adhesive has been related to a coiled-elongated shape conformation. The forces dominating this transition have been suggested to be controlled by the proteins polymeric architecture. However, the fact that 20% of VWF molecular weight originates from glycan moieties has so far been neglected in these calculations. In this study, we present a systematic experimental investigation on the role of N-glycosylation for VWF mediated platelet adhesion under flow. A microfluidic flow chamber with a stenotic compartment that allows one to mimic various physiological flow conditions was designed for the efficient analysis of the adhesion spectrum. Surprisingly, we found an increase in platelet adhesion with elevated shear rate, both qualitatively and quantitatively fully conserved when N-deglycosylated VWF (N-deg-VWF) instead of VWF was immobilized in the microfluidic channel. This has been demonstrated consistently over four orders of magnitude in shear rate. In contrast, when N-deg-VWF was added to the supernatant, an increase in adhesion rate by a factor of two was detected compared to the addition of wild-type VWF. It appears that once immobilized, the role of glycans is at least modified if not—as found here for the case of adhesion—negated. These findings strengthen the physical impact of the circulating polymer on shear dependent platelet adhesion events. At present, there is no theoretical explanation for an increase in platelet adhesion to VWF in the absence of its N-glycans. However, our data indicate that the effective solubility of the protein and hence its shape or conformation may be altered by the degree of glycosylation and is therefore a good candidate for modifying the forces required to uncoil this biopolymer. © 2013 AIP Publishing LLC. [<http://dx.doi.org/10.1063/1.4819746>]

### I. INTRODUCTION

The von Willebrand Factor (VWF) initiated platelet adhesion is a pivotal step for blood clot formation.<sup>1–9</sup> VWF is a large multimeric protein mainly secreted by endothelial cells (EC) to both plasma and the extracellular matrix of the subendothelial vessel wall.<sup>6–9</sup> Importantly, we have recently shown that VWF can be activated by hydrodynamic stress.<sup>10,11</sup> In a

<sup>a)</sup>M. A. Fallah and V. Huck contributed equally to this work.

<sup>b)</sup>Authors to whom correspondence should be addressed. Electronic addresses: stefan.schneider@medma.uni-heidelberg.de and mfs@bu.edu.

microfluidic setup, the biopolymer was exposed to increasing levels of shear rates, while simultaneously monitoring conformation and adhesion to the biofunctionalized channel bottom. Once a certain, critical wall shear stress was reached, the glycoprotein (polymer) reversibly transformed from a globular to a stretched conformation.<sup>10–12</sup> Simultaneously, the adhesion was strongly increased, presumably due to an increase in exposed binding sites upon stretching. This experiment solved a long known puzzle, namely the counterintuitive observation of increased platelet adhesion upon increasing wall shear.<sup>7,11</sup>

VWF is a glycoprotein, which contains oligosaccharide side chains making for approximately 20% of its molecular weight.<sup>13–16</sup> More specifically, 70% of these glycan moieties are N-linked glycans.<sup>17</sup> The oligosaccharide side chains are suggested to affect various properties of a given glycoprotein through its thermodynamical stability, in particular its solubility and/or its conformational behaviour.<sup>18</sup> For instance, it has been recently shown that N-glycans of VWF affect its interactions with ADAMTS13 modulator.<sup>19</sup> But decided studies to ascertain the pathophysiological impact of glycosylation defects or mutations are lacking so far. Processes of platelet adhesion and thrombus formation are directly affected by fluid dynamics within the circulatory system.<sup>20–24</sup> In some segments of the vascular system, e.g., small arterioles and arterial capillaries the wall shear rate estimates to be of the order of  $1700\text{ s}^{-1}$ .<sup>25</sup> However, in diseased arteries in which obstructive processes reduce the lumen diameter to 50%, shear rate can increase up to excess of  $5000\text{ s}^{-1}$ ; further occlusion up to 90% increases the shear rate up to dramatic levels.<sup>26</sup> This makes a geometrically constricted duct physiologically relevant for studying the VWF initiated platelet adhesion. While the relation between VWF and blood platelets immobilization is qualitatively well described, the ability of the protein to initiate thrombocyte adhesion at various wall shear rates has not been clearly quantified. Also, the role of the N-linked oligosaccharide in initiating platelet adhesion has remained unclear.

Driven by the mentioned requirements, we have designed and successfully implemented a microfluidic setup to study the VWF initiated platelet adhesion, both qualitatively and quantitatively. Microfluidics has proven to be a strong tool for *in vitro* investigation of complex biophysiological effects under dynamic conditions.<sup>27,28</sup> Here, a microchannel with a stenotic compartment is the core of this setup. Among other advantages, this microchannel also provides the technical advantage of simultaneously screening several flow- and shear-rates along the channel. Using the aforementioned setup, we have studied the effect of the N-deglycosylation of VWF (N-deg-VWF) on the protein's ability to initiate platelet adhesion. In particular, we have found out the impact of N-deglycosylation on both immobilized- and circulating- (plasmatic) VWF ability to initiate platelet adhesion under flow conditions over four orders of magnitude in shear rate. The increase in platelet adhesion with elevated shear of both immobilized N-deg-VWF and wild-type VWF was surprisingly conserved. In strong contrast, VWF initiated platelet adhesion was substantially increased with addition of N-deg-VWF to the supernatant, whereas further addition of wild-type VWF did not meaningfully affect the platelet adhesion rate.

## II. MATERIALS AND METHODS

### A. Microfluidic setup

The experimental setup is consisted of the flow channel driven by a high-precision syringe pump (NE-1000, New Era Pump Systems, Inc., NY, USA). The employed channel-geometry is a capped rectangular duct with a width of  $\approx 500\text{ }\mu\text{m}$  and height of  $\approx 60\text{ }\mu\text{m}$ . Within the stenosis, the width of the duct (along the y-axis) decreases to  $40\text{ }\mu\text{m}$ , whereas the height (along the z-axis) remains constant. A schematic two-dimensional and a three-dimensional projection are depicted in Figure 1. The geometrical structure of the channel was sketched using AUTOCAD software. This pattern was transferred to a mold by photolithography and the mold was filled with polydimethylsiloxane (PDMS, Dow Corning GmbH, Wiesbaden, Germany), a biocompatible transparent polymer, to obtain the desirable channel structure. Then, the PDMS channel was sealed to a glass slide by plasma oxidation and mounted onto an inverted microscope (Zeiss Axio Observer Z.1, Carl Zeiss AG, Oberkochen, Germany) capable of performing phase contrast-, fluorescence-, and reflection interference contrast-microscopy.

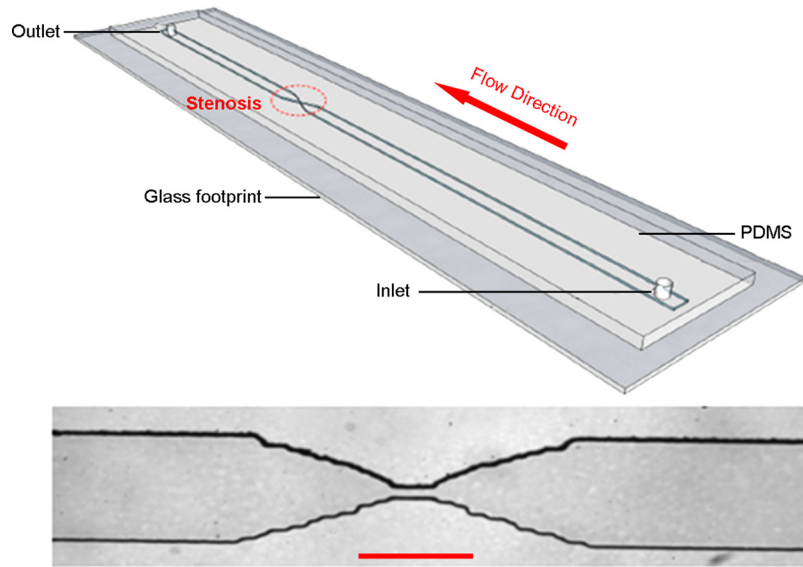


FIG. 1. Schematic sketch of the duct with a stenotic geometry and top view image of the stenotic channel. Scale bar corresponds to  $500\ \mu\text{m}$ .

## B. Fluid dynamics in the stenotic microchannel

For a rectangular channel the wall shear rate is obtained from the following equation:

$$\dot{\gamma}_w = \dot{\gamma}_a \frac{2}{3} \left( \frac{b^*}{f^*} + \frac{a^*}{f^*} \cdot \frac{1}{n} \right), \quad (1)$$

where  $a^*$ ,  $b^*$ , and  $f^*$  are geometric constants for a rectangular duct as defined in details in Son's work,  $n$  is the power law index and  $\dot{\gamma}_a$  is the apparent shear rate.<sup>29</sup> Assuming  $\Delta p = P_{\text{output}} - P_{\text{input}}$  to approximate the pressure drop, this equation can be used to calculate the wall shear rate within the neck of the microfluidic channel, where data acquisition and evaluation takes place as sketched schematically in Figure 2.

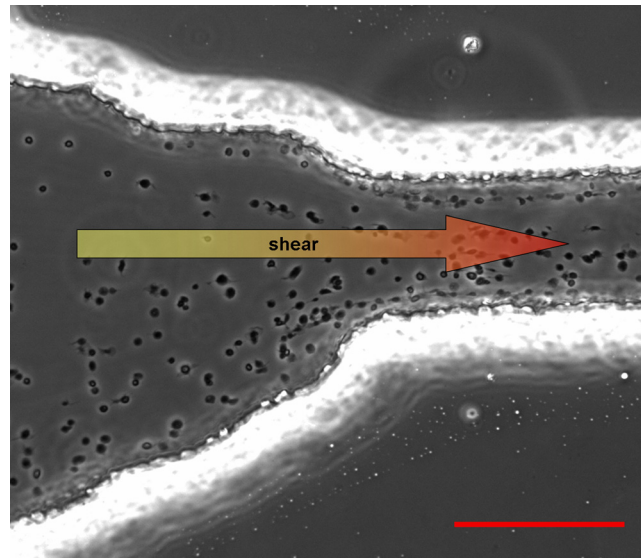


FIG. 2. Adhesion of thrombocytes to the footprint of a stenotic channel biofunctionalized with wild-type VWF. The number of adhered platelets per area increases along the channel length, toward the stenosis. The sharp decrease of the channel cross-section before stenosis provides a chance of screening various shear rates simultaneously at different compartments of a single channel. Scale bar corresponds to  $50\ \mu\text{m}$ .

Besides mimicking relevant physiological conditions,<sup>30,31</sup> the stenotic geometry provided a technical advantage over straight channel geometries, for instance, its sharp alternation of the duct's cross-section along the channel before and after the constricted compartment. A constant volumetric flow rate created by the syringe pump leads to various flow velocities and therefore to various wall shear rates along the channel for simultaneous observation (Fig. 2). To assure laminar flow conditions along the channel, the flow profile was studied by using polystyrene tracking beads (Polysciences, Inc. Warrington, PA, USA).

### C. N-deglycosylation of VWF

The N-linked oligosaccharides were detached from the main chain by digesting VWF with PNGase F (Peptide-N-glycosidase F) enzyme as previously described.<sup>19</sup> In brief, the enzyme released asparagine-linked oligosaccharides from glycoproteins and glycopeptides by hydrolyzing the amide of the asparagine (Asn) side chain.<sup>32–34</sup> Providing the necessary time and environment for the enzyme activity, treatment succeeds by removal of more than 90% of VWF N-linked glycans.<sup>19</sup>

### D. Biofunctionalization of the microchannels

In the capped planar geometry used biofunctionalization for different microfluidics patterns, becomes an easy task for even complex channel geometries. For biofunctionalization with VWF, fluorescent labeled (Alexa Fluor 488 protein labeling kit, Invitrogen, USA) VWF (500  $\mu\text{g}/\text{ml}$ , Department of Hematology, Imperial College London, UK) in TBS (Tris Buffered Saline) buffer solution was infused into the channel. In order to achieve an effective coating, we allowed the VWF in the solution to precipitate on glass the footprint of the duct for 3 h at 37 °C before beginning adhesion experiments. Channel biofunctionalization process with both the wild-type VWF and the N-deg-VWF was identical. Two control sets of channels were biofunctionalized with either collagen type I (10  $\mu\text{g}/\text{cm}^2$ , C7661, Sigma Aldrich, St. Louis, USA) as previously published<sup>35,36</sup> or 1% bovine serum albumin (BSA, Serva GmbH, Heidelberg, Germany) in HEPES buffered Ringer solution.

### E. Preparation of the supernatant

Blood from healthy volunteers was collected by using sodium citrate venous blood vacuum collection tubes. The study was conducted in conformity to the *Declaration of Helsinki*<sup>37</sup> and to *The International Conference on Harmonisation of Technical Requirements for Registration of Pharmaceuticals for Human Use (ICH)* Guidelines, available at <http://www.ich.org>, accessed in October 2010. It was approved by the Ethics Committee of the *Medical Faculty Mannheim, Heidelberg University* (Mannheim, Germany). Appropriate informed consent was obtained from all subjects. The monosodium citrate or the Acid Citrate Dextrose Solution (ACD) in citrate blood tubes acts as a reversible anticoagulant by blocking the calcium. Then, platelet rich plasma (PRP) with a platelet concentration of 200 000/ $\mu\text{l}$  was prepared for infusion into the biofunctionalized channels.

### F. Experimental design

Under physiological conditions, VWF comes into effect in both the extracellular matrix of the subendothelial vessel wall (immobilized) and the floating plasma (circulating).<sup>6,8,9,38</sup> In order to discretely study the effect of glycosylation of immobilized and circulating VWF on platelet adhesion, respectively, two sets of experiments have been designed. In the first set, channels were biofunctionalized with either VWF or N-deg-VWF as described above and perfused with PRP. In order to study the effect of the circulating VWF on platelet adhesion, we added either supplementary wild-type VWF or supplementary N-deg-VWF in a concentration of 20  $\mu\text{g}/\text{ml}$  to the PRP before starting the flow experiment; regardless of the supplementary circulating VWF, the channels were biofunctionalized with wild-type VWF. Various shear rates were swept consecutively from lower to higher values. Switching back to lower wall shear rates

has been frequently performed to control the reproducibility of the effects. To further elucidate the impact of the circulating VWF at higher and lower shear regimes, we performed control experiments using washed platelets as previously published<sup>39</sup> with or without supplementation of wild-type VWF in a biofunctionalized planar microfluidic channel system (BioFlux, San Francisco, CA, USA). Then, VWF mediated thrombocyte adhesion to the coated glass footprint of the channel was studied under various flow conditions, captured by a CCD camera (AxioCam MrM, Zeiss AG, Jena, Germany). Platelet adhesion was investigated at various shear rates for four minutes for each of the aforementioned settings at least by three independent experiments. All experiments were conducted at 37 °C.

### G. Statistical analysis

Mean data of experiments are given with standard deviation (SD). Statistical computation was performed with SAS 9.2 (SAS Institute Inc., Cary, North Carolina, USA).

## III. RESULTS AND DISCUSSION

Although the cascade of complex interactions from platelet activation, aggregation, and thrombus formation is qualitatively well studied,<sup>35,38,40,41</sup> a systematic screening of the specific interaction of immobilized and circulating VWF and thrombocytes (VWF initiated platelet arrest) and the impact of VWF glycosylation has so far not been provided. This also calls for reducing the system to its main players. Those are on one hand the circulating VWF and the platelets in blood plasma, on the other hand, the immobilized VWF exposed to the bloodstream. The PRP contains the former two of the players, the biofunctional channel coat can mimic the latter. Our microfluidic setup allows for a laminar PRP flow inside the channel within the whole physiologically relevant shear values.

### A. Platelet adhesion and the immobilized VWF

Under pathophysiological conditions, immobilized VWF is exposed to the blood from dissected subendothelial extracellular matrix at the site of vessel injuries or from the luminal side of intact activated endothelium.<sup>9,36</sup> Focusing on the role of this immobilized VWF, platelet adhesion remains surprisingly conserved when the  $\mu$ -channel was biofunctionalized with N-deg-VWF (Fig. 3, red curve) instead of wild-type VWF (Fig. 3, black curve). We found a clear shear rate dependency of the VWF mediated platelet adhesion to both the immobilized wild-type VWF and the N-deg-VWF. The adhesion rate increases steadily with rise of shear rate to up to  $20\,000\text{ s}^{-1}$ . However, the adhesion starts to experience a decline at shear rates above  $20\,000\text{ s}^{-1}$ .

Control experiments have been performed by biofunctionalization of the  $\mu$ -channel with either Collagen type I or BSA (data not shown). The irreversible adhesion of blood platelets to the immobilized matrix protein collagen type I has been found to be of extremely low magnitude. At shear rate below  $1000\text{ s}^{-1}$  only single platelets reversibly interacted with the collagen coat. Increasing shear rate to  $1000\text{ s}^{-1}$  and above, the adhered platelets detach. The BSA coat did not support platelet adhesion.

The observed shear force dependency of platelet adhesion becomes even more impressive considering the fact that the PRP is a Newtonian fluid, in which the Fahraeus-Lindquist effect vanishes.<sup>42</sup> Under physiological conditions of whole blood, the Red Blood Cells (RBCs) press the platelets towards the walls of the circulatory system. This provides a very high local concentration of the platelets in vicinity of the walls. In our setup since the RBCs were absent and the laminar flow condition kept most of the platelets off the wall, a much smaller number of platelets came into direct contact with the wall than in the microcirculatory system. However, one has to take in consideration that this finding does not clarify the role of the circulating plasma VWF on platelet adhesion.

### B. Platelet adhesion and the circulating VWF

PRP naturally contains a concentration of  $\sim 10\text{ }\mu\text{g/ml}$  circulating (plasmatic) VWF.<sup>9</sup> We increased the concentration of the circulating VWF nearly to two times of the natural

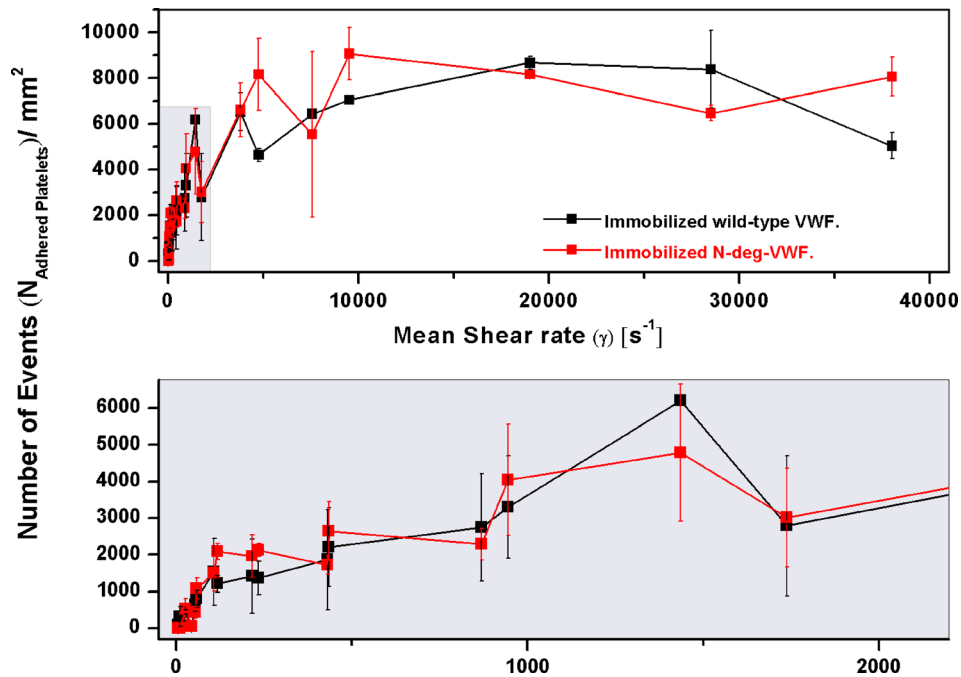


FIG. 3. Black curve: Adhesion rate of thrombocytes (number/mm<sup>2</sup>) to the immobilized VWF. Red curve: adhesion rate of platelets to the immobilized N-deg-VWF. The VWF mediated platelet adhesion remains conserved when the duct is bio-functionalized with N-deg-VWF instead of wild-type VWF. The VWF mediated platelet adhesion shows a shear dependent behavior over four orders of magnitude of shear rate. The platelet adhesion rate at lower shear values (grey box) is shown below in detail.

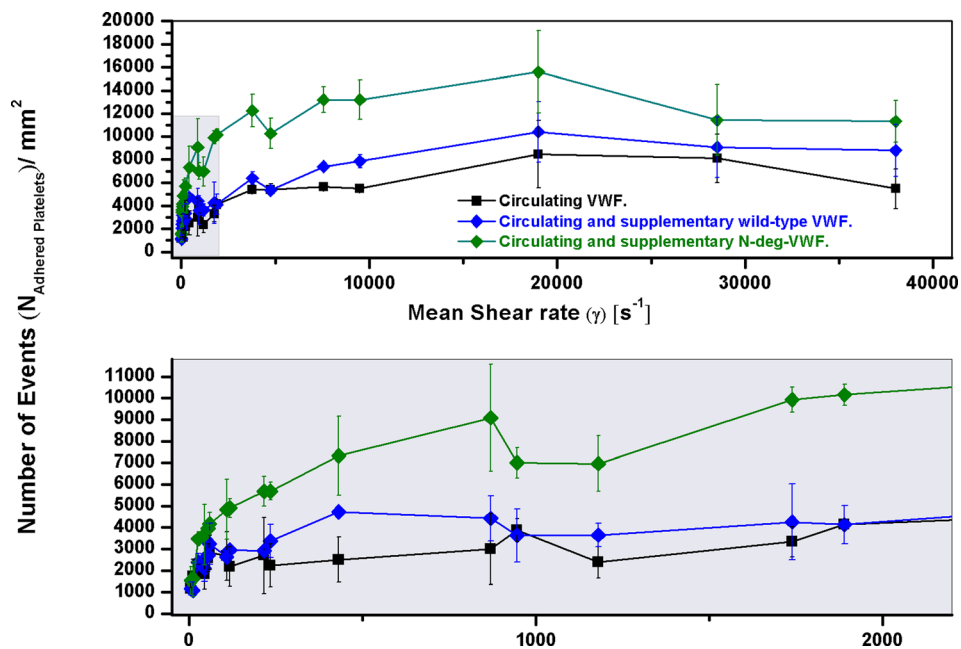


FIG. 4. Black curve: Adhesion rate of thrombocytes (number/mm<sup>2</sup>) to the immobilized VWF in presence of just the natural circulating VWF. Blue curve: adhesion rate of platelets to the immobilized VWF in presence of extra circulating wild-type VWF in the supernatant; the supplementary circulating wild-type VWF does not enhance the platelet adhesion meaningfully. Green curve: Adhesion rate of platelets (number/mm<sup>2</sup>) to the immobilized VWF in presence of extra circulating N-deg-VWF; the supplementary circulating N-deg-VWF increases the VWF mediated platelet adhesion by a factor of two. The platelet adhesion rate at lower shear values (grey box) is shown below in detail.

level by adding supplementary wild-type VWF and supplementary N-deg-VWF to the PRP, respectively. Increasing the circulating VWF content by adding wild-type VWF to the supernatant did not meaningfully impact the VWF mediated adhesion in our experimental setting as shown in Figure 4 (blue curve vs. black curve). In strong contrast, adding supplementary N-deg-VWF to the supernatant forced up the VWF mediated platelet adhesion by a factor of two (Fig. 4, green curve). The exact mechanism of this effect is still unknown. However, it is likely that glycosylation of a protein affects its thermodynamic behaviour and stability.<sup>18</sup> Here, one could hypothesize; that removal of glycans reduces the force required inducing the coiled-stretched transition of VWF, for instance, by modifying the effective solubility of the protein. As a result, N-deglycosylation of the floating VWF is promoting the flow driven exposure of VWF domains responsible for platelet adhesion.

Furthermore, Figure 4 implies that at higher shear rates the circulating VWF would be more dominant for initiating the platelet adhesion than the immobilized. In order to investigate this assumption, we have performed a set of control experiments. To focus on the impact of circulating VWF on the shear dependency of thrombocyte adhesion, we perfused wild-type VWF-biofunctionalized microchannels with stained, washed platelets instead of PRP without any content of circulating VWF in comparison to platelet solution supplemented with 10  $\mu\text{g}/\text{ml}$  wild-type VWF. As shown in Figure 5, there was no difference in the number of adhesion events under moderate shear conditions up to 2500  $\text{s}^{-1}$ . Raising the shear rates above 5000  $\text{s}^{-1}$  led to an increase of adhered platelets in the circulating VWF containing group became more impressive under high shear conditions of 20 000  $\text{s}^{-1}$ .

Only in the presence of a minimum of 10  $\mu\text{g}/\text{ml}$  circulating VWF this shear dependent increase of adhesion event was observable, whereas further elevation of the circulating VWF

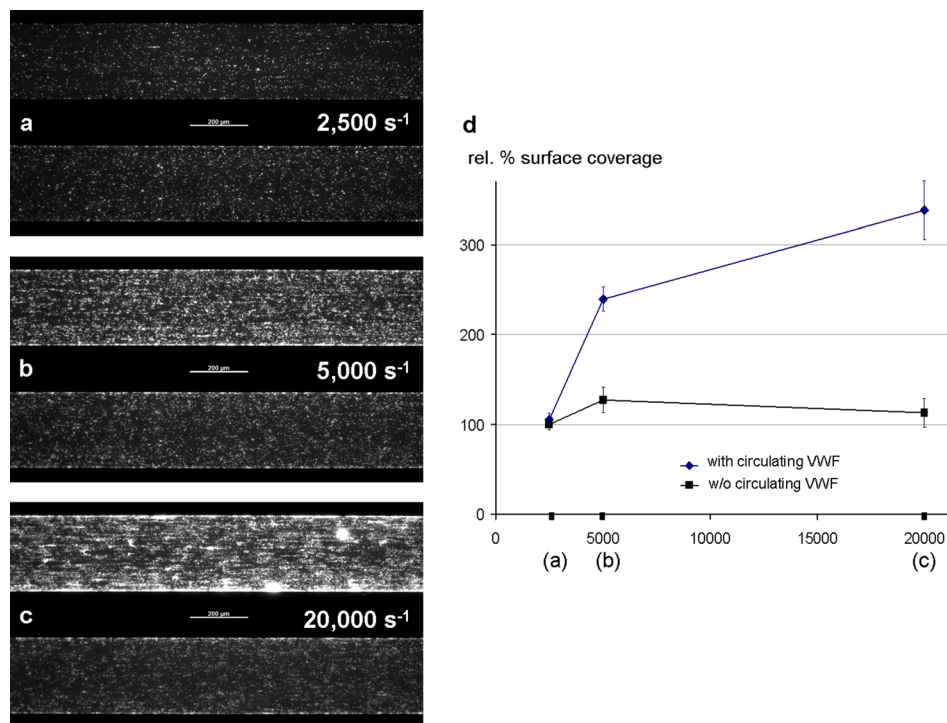


FIG. 5. Adhesion of washed and stained platelets to the footprint of a planar microfluidic channel system biofunctionalized with wild-type VWF. The upper channels of (a), (b), and (c) are supplemented with 10  $\mu\text{g}/\text{ml}$  circulating VWF, in the lower channels no circulating VWF is present. The surface coverage representing the number of adhered platelets per area is identical with and without circulating VWF at 2500  $\text{s}^{-1}$  (a). Raising the shear rates to 5000  $\text{s}^{-1}$  leads to an increase of adhered platelets only in the circulating VWF containing channel (b), become more impressive under high shear conditions in a range of 20 000  $\text{s}^{-1}$  (c). Scale bars correspond to 200  $\mu\text{m}$ .

concentration did not affect the shear dependent characteristics of platelets adhesion (data not shown).

#### IV. CONCLUSIONS

We have designed a microfluidic device which mimics the complex geometry and fluid dynamics of our microcirculation and allows, together with some further technical advancements, for a systematic study of thrombotic activities. From the biomimetic point of view, we have successfully designed and implemented a stenosis microchannel for the efficient analysis of the physiologically relevant adhesion spectrum. From a biological point of view, we have shown the impact of N-linked glycans on the ability of VWF to mediate platelet adhesion both in the immobilized and the circulating state. Surprisingly, we found that the increase in platelet adhesion with elevated shear rate is qualitatively and quantitatively fully conserved when N-deg-VWF instead of wild-type VWF was immobilized in the microfluidic channel. Addition of supplementary wild-type VWF to the circulating PRP did not affect platelet adhesion. In the contrary, the supplementary N-deg-VWF added to the supernatant triggered an increase in adhesion rate by a factor of two. These findings considerably strengthen the physical impact of circulating VWF on shear dependent platelet adhesion demonstrated consistently over four orders of magnitude in shear rate.

It appears that once circulating, the effect of removing glycans on conformational properties of the glycoprotein is entirely different than under immobilization. Although this suggests, that N-linked oligosaccharide side chains are good candidates for modifying the forces required to uncoil this biopolymer, this study also demonstrates the little understanding we have for the physical role of glycosylation and will hopefully foster new theoretical activities in this field. One way of thinking we will explore in the future is to consider VWF as a thermodynamic system, which is characterized by its diagram of state. In such a unified picture glycosylation will become a thermodynamic parameter just as pH, temperature, or ion concentrations.

#### ACKNOWLEDGMENTS

The authors acknowledge kind support from the German Research Foundation (DFG) SHENC—Research Unit FOR1543 (SWS/VH project A2, AW/MAF project B1 and MFS for a Guest Professorship).

Hereby, the authors declare that they have no relevant conflicts of interest.

- <sup>1</sup>H. Cheng, R. Yan, S. Li, Y. Yuan, J. Liu, C. Ruan, and K. Dai, *Am. J. Physiol. Heart Circ. Physiol.* **297**(6), H2128 (2009).
- <sup>2</sup>E. Hanson, K. Jood, S. Karlsson, S. Nilsson, C. Blomstrand, and C. Jern, *J. Thromb. Haemost.* **9**(2), 275 (2011).
- <sup>3</sup>P. M. Mannucci, *Arterioscler., Thromb., Vasc. Biol.* **18**(9), 1359 (1998).
- <sup>4</sup>G. L. Mendolicchio and Z. M. Ruggeri, *Semin Hematol.* **42**(1), 5 (2005).
- <sup>5</sup>R. Moroose and L. W. Hoyer, *Annu. Rev. Med.* **37**, 157 (1986).
- <sup>6</sup>Z. M. Ruggeri, *Best Pract. Res. Clin. Haematol.* **14**(2), 257 (2001).
- <sup>7</sup>Z. M. Ruggeri, *Thromb. Res.* **120**(Suppl 1), S5 (2007).
- <sup>8</sup>Z. M. Ruggeri, J. N. Orje, R. Habermann, A. B. Federici, and A. J. Reininger, *Blood* **108**(6), 1903 (2006).
- <sup>9</sup>J. E. Sadler, *Annu. Rev. Biochem.* **67**, 395 (1998).
- <sup>10</sup>A. Alexander-Katz, M. F. Schneider, S. W. Schneider, A. Wixforth, and R. R. Netz, *Phys. Rev. Lett.* **97**(13), 138101 (2006).
- <sup>11</sup>S. W. Schneider, S. Nuschele, A. Wixforth, C. Gorzelanny, A. Alexander-Katz, R. R. Netz, and M. F. Schneider, *Proc. Natl. Acad. Sci. U.S.A.* **104**(19), 7899 (2007).
- <sup>12</sup>I. Singh, E. Themistou, L. Porcar, and S. Neelamegham, *Biophys. J.* **96**(6), 2313 (2009).
- <sup>13</sup>P. Y. Bruice, *Organic Chemistry* (Prentice-Hall Inc., Pearson Education, 2001).
- <sup>14</sup>T. Matsui, K. Titani, and T. Mizuochi, *J. Biol. Chem.* **267**(13), 8723 (1992).
- <sup>15</sup>C. M. Millar and S. A. Brown, *Blood Rev.* **20**(2), 83 (2006).
- <sup>16</sup>K. Titani, S. Kumar, K. Takio, L. H. Ericsson, R. D. Wade, K. Ashida, K. A. Walsh, M. W. Chopek, J. E. Sadler, and K. Fujikawa, *Biochemistry (Mosc)* **25**(11), 3171 (1986).
- <sup>17</sup>B. Samor, C. Mazurier, M. Goudemand, P. Debeire, B. Fournet, and J. Montreuil, *Thromb. Res.* **25**(1–2), 81 (1982).
- <sup>18</sup>D. Shental-Bechor and Y. Levy, *Proc. Natl. Acad. Sci. U.S.A.* **105**(24), 8256 (2008).
- <sup>19</sup>T. A. McKinnon, A. C. Chion, A. J. Millington, D. A. Lane, and M. A. Laffan, *Blood* **111**(6), 3042 (2008).
- <sup>20</sup>P. Andre, P. Hainaud, C. Bal dit Sollier, L. I. Garfinkel, J. P. Caen, and L. O. Drouet, *Arterioscler., Thromb., Vasc. Biol.* **17**(5), 919 (1997).
- <sup>21</sup>L. F. Morton, B. Griffin, D. S. Pepper, and M. J. Barnes, *Thromb. Res.* **32**(6), 545 (1983).
- <sup>22</sup>Z. M. Ruggeri, *Nat. Med.* **8**(11), 1227 (2002).

- <sup>23</sup>K. S. Sakariassen, P. A. Bolhuis, and J. J. Sixma, *Nature* **279**(5714), 636 (1979).
- <sup>24</sup>B. Savage, F. Almus-Jacobs, and Z. M. Ruggeri, *Cell* **94**(5), 657 (1998).
- <sup>25</sup>G. J. Tangelder, D. W. Slaaf, T. Arts, and R. S. Reneman, *Am. J. Physiol.* **254**(6 Pt 2), H1059 (1988).
- <sup>26</sup>L. D. Back, J. R. Radbill, and D. W. Crawford, *J. Biomech.* **10**(5–6), 339 (1977).
- <sup>27</sup>A. Karimi, S. Yazdi, and A. M. Ardekani, *Biomicrofluidics* **7**(2), 021501 (2013).
- <sup>28</sup>N. Piacentini, G. Mernier, R. Tornay, and P. Renaud, *Biomicrofluidics* **5**(3), 34122 (2011).
- <sup>29</sup>Y. Son, *Polymer* **48**(2), 632 (2007).
- <sup>30</sup>H. Hikita, A. Sato, T. Nozato, T. Kawashima, Y. Takahashi, T. Kuwahara, and A. Takahashi, *Scand. Cardiovasc. J.* **43**(5), 298 (2009).
- <sup>31</sup>A. Jeremias, B. Sylvia, J. Bridges, A. J. Kirtane, B. Bigelow, D. S. Pinto, K. K. Ho, D. J. Cohen, L. A. Garcia, D. E. Cutlip, and J. P. Carrozza, Jr., *Circulation* **109**(16), 1930 (2004).
- <sup>32</sup>J. Q. Fan and Y. C. Lee, *J. Biol. Chem.* **272**(43), 27058 (1997).
- <sup>33</sup>A. L. Tarentino, C. M. Gomez, and T. H. Plummer, Jr., *Biochemistry (Mosc)* **24**(17), 4665 (1985).
- <sup>34</sup>A. L. Tarentino and T. H. Plummer, Jr., *Methods Enzymol.* **230**, 44 (1994).
- <sup>35</sup>A. Barg, R. Ossig, T. Goerge, M. F. Schneider, H. Schillers, H. Oberleithner, and S. W. Schneider, *Haemost.* **97**(4), 514 (2007).
- <sup>36</sup>T. Colace, E. Falls, X. L. Zheng, and S. L. Diamond, *Ann. Biomed. Eng.* **39**(2), 922 (2011).
- <sup>37</sup>P. P. Rickham, *Br. Med. J.* **2**(5402), 177 (1964).
- <sup>38</sup>A. S. Fauci, E. Braunwald, D. L. Kasper, S. L. Hauser, D. L. Longo, J. L. Jameson, and J. Loscalzo, *Harrison's Principles of Internal Medicine* (McGraw-Hill Professional, 2008).
- <sup>39</sup>K. De Ceunynck, S. Rocha, H. B. Feys, S. F. De Meyer, H. Uji-i, H. Deckmyn, J. Hofkens, and K. Vanhoorelbeke, *J. Biol. Chem.* **286**(42), 36361 (2011).
- <sup>40</sup>E. W. Merrill, E. R. Gilliland, G. Cokelet, H. Shin, A. Britten, and R. E. Wells, Jr., *J. Appl. Physiol.* **18**, 255 (1963).
- <sup>41</sup>E. Tolouei, C. J. Butler, A. Fouras, K. Ryan, G. J. Sheard, and J. Carberry, *Ann. Biomed. Eng.* **39**(5), 1403 (2011).
- <sup>42</sup>R. Fahraeus and T. Lindqvist, *Am. J. Physiol.* **96**, 562 (1931).